Fluorescence Correlation Spectroscopy: Novel Variations of an Established Technique

Elke Haustein and Petra Schwille

BioTec TU Dresden, Institute for Biophysics, D-01307 Dresden, Germany;
email: Elke.haustein@biotec.tu-dresden.de; Petra.schwille@biotec.tu-dresden.de

Annu. Rev. Biophys. Biomol. Struct. 2007.
36:151–69

The *Annual Review of Biophysics and Biomolecular Structure* is online at biophys.annualreviews.org

This article's doi:
10.1146/annurev.biophys.36.040306.132612

1056-8700/07/0609-0151$20.00

Key Words

fluctuation, autocorrelation, cross-correlation, one-photon excitation, multiphoton excitation, single molecule

Abstract

Fluorescence correlation spectroscopy (FCS) is one of the major biophysical techniques used for unraveling molecular interactions in vitro and in vivo. It allows minimally invasive study of dynamic processes in biological specimens with extremely high temporal and spatial resolution. By recording and correlating the fluorescence fluctuations of single labeled molecules through the exciting laser beam, FCS gives information on molecular mobility and photophysical and photochemical reactions. By using dual-color fluorescence cross-correlation, highly specific binding studies can be performed. These have been extended to four reaction partners accessible by multicolor applications. Alternative detection schemes shift accessible time frames to slower processes (e.g., scanning FCS) or higher concentrations (e.g., TIR–FCS). Despite its long tradition, FCS is by no means dated. Rather, it has proven to be a highly versatile technique that can easily be adapted to solve specific biological questions, and it continues to find exciting applications in biology and medicine.

Contents

INTRODUCTION

FCS: fluorescence correlation spectroscopy

OPE: one-photon excitation

The need for better, minimally invasive diagnostic tools and more specialized instrumentation to answer highly specific biological questions has triggered an avalanche in fluorescence-based technique development. Fluorescence correlation spectroscopy (FCS) is one of the many different modes of high-resolution spatial and temporal analysis of extremely dilute biomolecules.

FCS was developed in the early 1970s (26, 59, 60) as a miniaturization of dynamic light scattering. The novel concept of FCS is to take advantage of the minute spontaneous fluctuations in fluorescence emission of the molecules in thermodynamic equilibrium. First, FCS was applied to measure diffusion and chemical kinetics of DNA-drug intercalation (59, 60). Following these proof-of-principle measurements, a variety of studies have been devoted to the investigation of particle concentration and mobility (29) and even cellular measurements (27). To enhance detection sensitivity and background suppression, Rigler et al. (72) combined FCS with a confocal setup. In the following years, the analytical and diagnostic potential of FCS was demonstrated. FCS was successfully applied to study binding of nucleic acids (47) and proteins (69). Moreover, a multitude of environmental effects inducing fluctuations in the fluorescence yield of single dye molecules could be studied, including, for example, reversible protonation (32) but also electron transfer or even oxygen and ion concentrations (37).

However, in turbid media and in cells the signal-to-noise ratio is influenced by autofluorescence and scattering. Because of the inherent depth discrimination, two-photon excitation (TPE) was suggested as an alternative, at the same time reducing out-of-focus photobleaching. In 1995 the first two-photon-FCS experiments in cells were reported (9).

The detection specificity for bimolecular reactions was significantly enhanced by introducing dual-color cross-correlation schemes for the simultaneous observation of different fluorescent species, first for one-photon excitation (OPE) in 1997 (77) and then for TPE in 2002 (35). At present, intracellular FCS applications probing the in situ dynamics of fluorescent probes experience a rapidly growing popularity. Nevertheless, the increasing complexity of the biological systems under investigation also causes a virtual explosion in the development and refinement of different methods that still belong to the generic concept of FCS.

SOME FLUORESCENT DYES

As most biologically relevant molecules are nonfluorescent, a necessary prerequisite consists in labeling the particle to be investigated. Autofluorescent proteins can be incorporated into proteins by genetic fusion. Their most prominent representatives belong to the green fluorescent protein (GFP) family, originally isolated from the jellyfish *Aequorea victoria*. Only recently were monomeric forms of longer-wavelength-emitting proteins created, e.g., mRFP1 (15) or mCherry (78). All known autofluorescent proteins are relatively large (~27 kDa). If size matters, organic fluorophores such as fluorescein and rhodamine, and especially their enhanced derivatives, are

a good option. Available in a wide range of colors, these small dyes (~1 kDa) minimize steric hindrance.

Quantum dots (QDs) are nanocrystalline semiconductor particles (core diameter, ~2–10 nm) and feature exceptional photostability, narrow emission spectra, and huge two-photon-action cross-sections (53). Biocompatibility was increased to allow long-term, multicolor imaging of live cells and even FCS (53).

EXPERIMENTAL SETUP

A custom-built FCS setup can easily be realized on the basis of an inverted microscope using one of the side ports for FCS detection (**Figure 1**). One or more parallel laser beams are directed via a dichroic mirror onto the back-aperture of a water immersion objective with high numerical aperture (NA > 0.9). The red-shifted fluorescence from the sample is collected by the same objective and transmitted by the dichroic and the emission filters.

QD: quantum dot

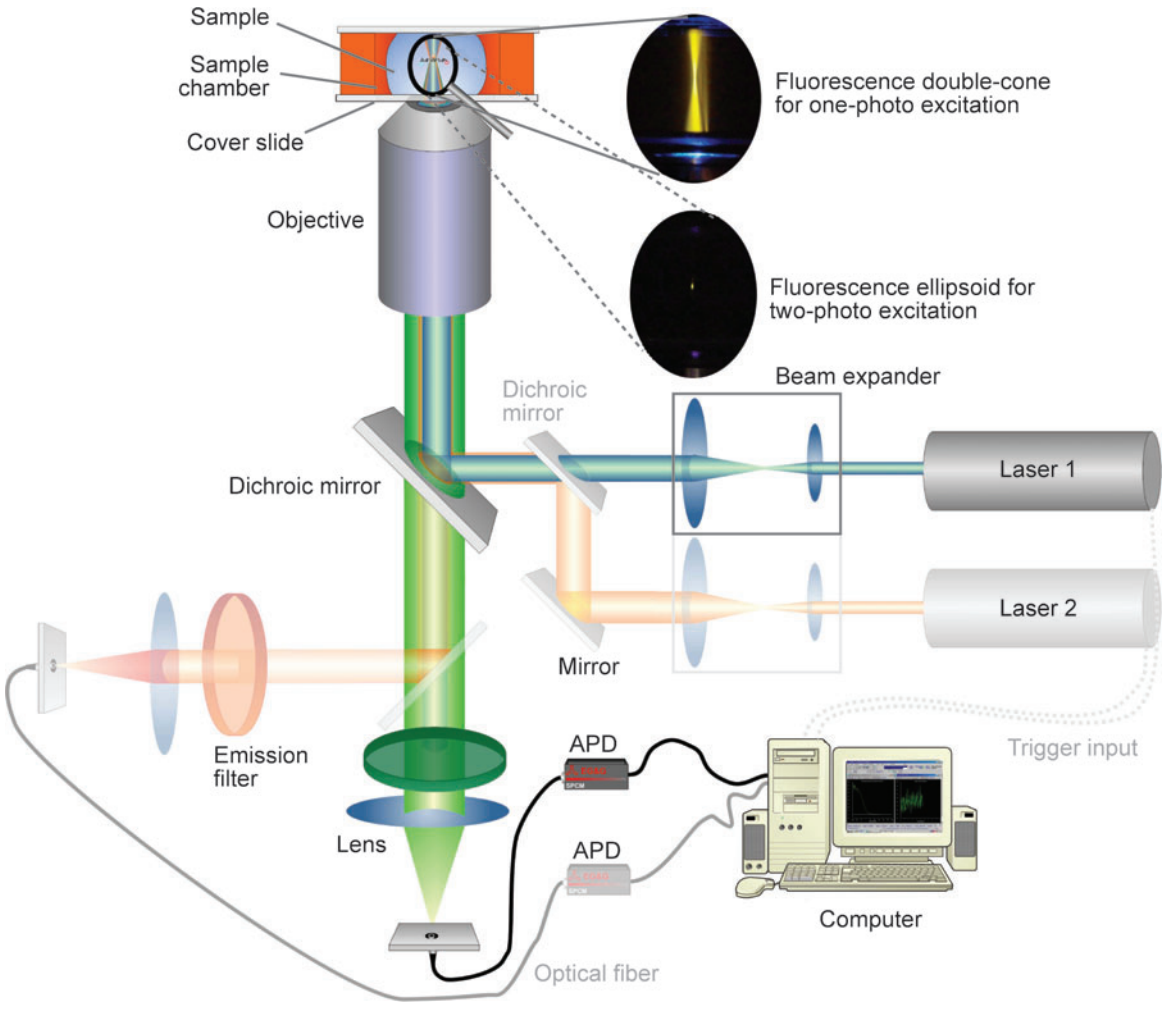

Figure 1

Schematic experimental setup for single-channel measurements (*blue-green excitation* and *green detection channel*) or dual-color cross-correlation (*green* and *red beampaths*). The shape of the focal volume depends on the excitation mode.

APD: avalanche photodiode

A confocal pinhole of variable diameter (30–100 μm) in the image plane (field aperture) ensures axial resolution for OPE (for details see References 33 and 36). The entrance aperture of a multimode optical fiber may be a substitute for the pinhole, as detectors, photomultiplier tubes, or avalanche photodiodes (APDs) with single-photon sensitivity can be used. The signal is then correlated by a multiple-tau hardware correlator (e.g., ALV, Langen, Germany, or **http://www.correlator.com/**) with quasi-logarithmic lag times or by using software correlation. Evaluation of the curves can be carried out by the Levenberg-Marquardt nonlinear least-square fitting routine.

FCS: THEORETICAL OUTLINE

Autocorrelation

Tiny fluctuations in the fluorescence signal from the excited molecules in the focal volume are incessantly occurring at ambient temperatures. This noise can be quantified by temporally autocorrelating the recorded intensity signal. The normalized autocorrelation function for the fluorescence fluctuations $\delta F(t)$ of the signal $F(t)$ is defined as

$$G(\tau) = \frac{\langle F(t)\cdot F(t+\tau)\rangle}{\langle F(t)\rangle^2} = \frac{\langle \delta F(t)\cdot \delta F(t+\tau)\rangle}{\langle F(t)\rangle^2} + 1, \qquad 1.$$

with

$$\delta F(t) = F(t) - \langle F(t)\rangle$$

$$\text{and} \quad \langle F(t)\rangle = \frac{1}{T}\int_0^T F(t)dt. \qquad 2.$$

Because the relative fluctuations become smaller with increasing numbers of measured particles, it is important to minimize the average number of molecules in the focal volume to between 0.1 and 1000. Corresponding concentrations range from subnanomolar ($\sim 10^{-10}$ M) to (sub)micromolar ($\sim 10^{-6}$ M) for a focal volume of about 1 femtoliter.

Mobility. A detailed derivation of the correlation functions can be found, for example, in References 4 and 26. Considering only free diffusion for a single species, the autocorrelation function reads:

$$G_{3D}(\tau) = \underbrace{\frac{1}{V_{eff}\cdot\langle C\rangle}}_{=\frac{1}{\langle N\rangle}} \cdot \left(\frac{1}{1+\frac{\tau}{\tau_D}}\cdot\frac{1}{\sqrt{1+\frac{r_0^2}{z_0^2}\cdot\frac{\tau}{\tau_D}}}\right). \qquad 3.$$

The first factor in Equation 3 is exactly the inverse of the average particle number in the focal volume, so that the local concentration can be determined directly from the amplitude G(0). The most common model for the observation volume is a three-dimensional Gaussian intensity profile (4). The $1/e^2$ radius is given by r_0, whereas it is z_0 in the axial direction. The lateral diffusion time τ_D that a molecule stays in the focal volume can be expressed in terms of the diffusion coefficient D:

$$\tau_D = \frac{r_0^2}{\alpha\cdot D}, \qquad 4.$$

where α equals 4 for OPE and 8 for TPE. The autocorrelation function for two-dimensional diffusion, for example, in a membrane reads (26):

$$G_{2D}(\tau) = \frac{1}{N}\cdot\frac{1}{1+\frac{\tau}{\tau_D}}. \qquad 5.$$

Molecules can also be actively transported through the focal volume (61). If considering no chemical reactions and only one species, the diffusion autocorrelation function is weighted by an exponential term describing the directed flow with velocity $\vec{v}$:

$$G_{flow}(\tau) = \frac{1}{V_{eff}\cdot\langle C\rangle}\cdot\frac{1}{1+\frac{\tau}{\tau_D}}\cdot\frac{1}{\sqrt{1+\frac{r_0^2}{z_0^2}\cdot\frac{\tau}{\tau_D}}} \cdot e^{-\left(\frac{(v_x^2+v_y^2)\cdot\tau^2}{r_0^2}\right)\cdot\left(\frac{1}{1+\frac{\tau}{\tau_D}}\right)} \cdot e^{-\left(\frac{(v_z^2)\cdot\tau^2}{z_0^2}\right)\cdot\left(\frac{1}{1+\frac{r_0^2}{z_0^2}\cdot\frac{\tau}{\tau_D}}\right)}. \qquad 6.$$

Especially in cells the distinction between directed and random motion can be crucial

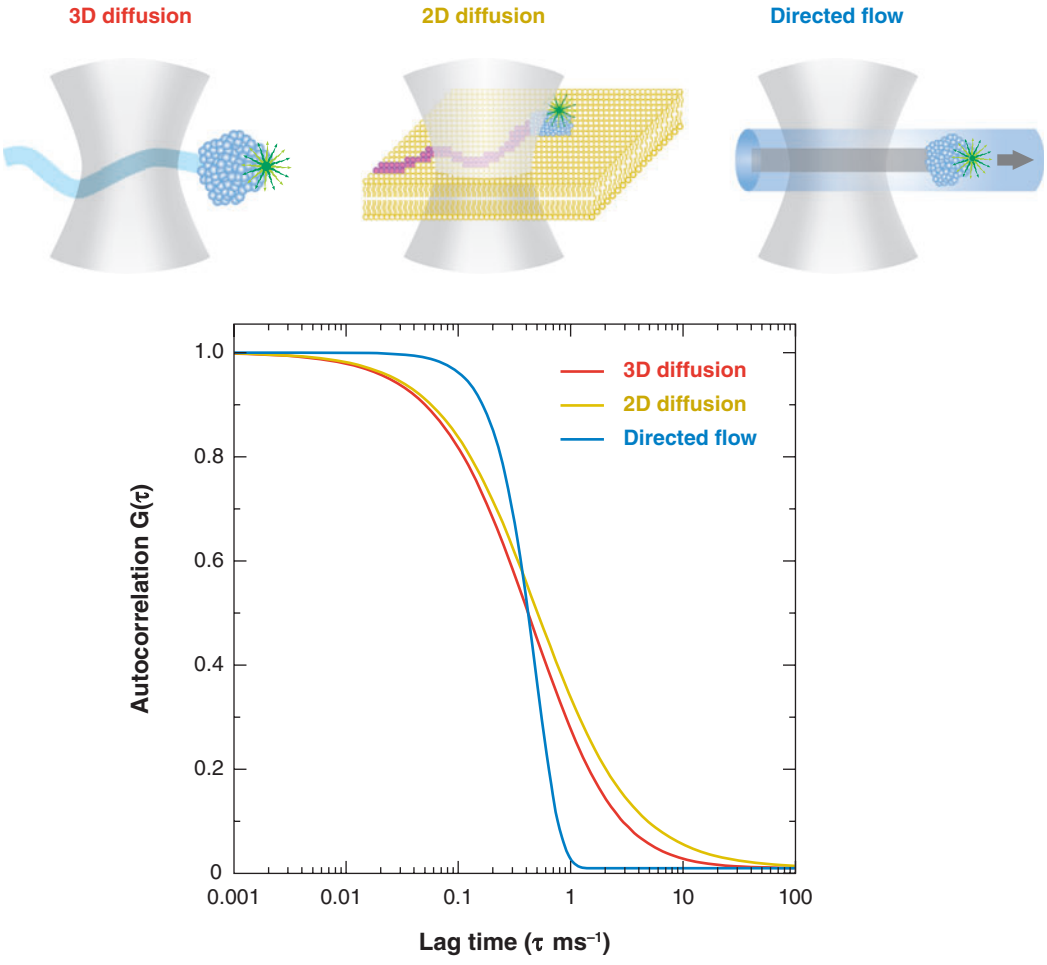

Figure 2

Model autocorrelation curves for different kinds of particle motion: free diffusion in three dimensions (*red*), free diffusion in two dimensions, e.g., for membrane-bound molecules (*yellow*) and directed flow (*cyan*).

for understanding the underlying processes (**Figure 2**). For several species of independently diffusing particles, the autocorrelation function is given by the sum of the correlation functions for the individual species weighted by the square of the fractional intensity.

Unimolecular reactions. In addition, the fluorescence properties of the chromophore may change while it is traversing the laser focus. The most common cause for such a flickering in the fluorescence intensity is the transition of the dye to the first excited triplet state. The normalized autocorrelation function for diffusion and a unimolecular reaction that does not influence the diffusion characteristics then reads (85):

$$G_{unimol}(\tau) = G_{diff}(\tau) \cdot G_{blink}(\tau). \qquad 7.$$

Typically, the triplet blinking mentioned above is described by a simple exponential decay visible as an additional shoulder in the measured curves:

$$G_{triplet}(\tau) = \cdot 1 + \frac{T}{1-T} \cdot e^{-\frac{\tau}{\tau_{triplet}}}. \qquad 8.$$

Cross-Correlation

Looking out for common features of two independently measured signals, F_i and F_j, one can generalize Equation 1:

$$G_x(\tau) = \frac{\langle \delta F_i(t) \cdot \delta F_j(t+\tau) \rangle}{\langle F_i(t) \rangle \cdot \langle F_j(t) \rangle}. \qquad 9.$$

Assuming ideal conditions, in which both channels have the same effective volume element V_{eff}, fully separable emission spectra, and a negligible emission-absorption overlap integral, the following correlation curves can be derived:

Autocorrelation:

$$G_{i,j}(\tau) = \frac{\left(\langle C_{i,j} \rangle M_i(\tau) + \langle C_{ij} \rangle M_{ij}(\tau) \right)}{V_{eff}(\langle C_{i,j} \rangle + \langle C_{ij} \rangle)^2}; \qquad 10.$$

Cross-correlation:

$$G_\times(\tau) = \frac{\langle C_{ij} \rangle M_{ij}(\tau)}{V_{eff}(\langle C_i \rangle + \langle C_{ij} \rangle)(\langle C_j \rangle + \langle C_{ij} \rangle)}, \qquad 11.$$

where $M_{ij}(\tau)$ is the motion-related part of the correlation function. More complicated situations are discussed in Reference 36. The amplitude of the cross-correlation function is directly proportional to the concentration of double-labeled particles:

$$\langle C_{ij} \rangle = \frac{G_\times(0)}{G_i(0) \cdot G_j(0) \cdot V_{eff}}. \qquad 12.$$

APPLICATIONS

Single-Channel Applications

The most basic form of an FCS setup consists of only one excitation wavelength and a single detection channel.

Concentrations. In highly dilute solutions, the nominal concentration may be much higher than the actual concentration of the molecules of interest in the sample chamber, because adsorption processes dominate in the nanomolar regime. To determine exact binding coefficients, knowledge of the local concentrations is crucial. As the amplitude of the autocorrelation curve is inversely proportional to the average number of fluorescent molecules in the observation volume, FCS is ideally suited to determine concentrations, especially relative values. Charier et al. (16) measured local reactant concentrations of specific, pH-sensitive fluorescent probes. They also examined the conditions under which FCS is considered a superior tool to measure concentrations of specially tailored fluorescent probes for use as calibration-free pH sensors. It is even possible to use the concentration dependence of the autocorrelation amplitude to investigate the particle size of aggregates or lipid micelles (87).

Mobility studies. Although the accuracy of values derived for the diffusion coefficient may vary (28), it is more straightforward to address directly the mobility of particles.

Size. The diffusion coefficient is related to the hydrodynamic radius of the (spherical) particle in solution by the Stokes-Einstein equation, so that the particle size can be estimated:

$$D_i = \frac{kT}{6\pi \eta_V R_{h,i}}, \qquad 13.$$

where η_V is the viscosity of the medium, T is the temperature, and k is the Boltzmann constant. Thus, the diffusion coefficient is inversely proportional to the hydrodynamic radius $R_{h,i}$ of the particles. In this way water-soluble QDs were shown to have larger apparent diameters in water than when recorded by electron microscopy, potentially due to an additional hydration shell (88). A more comprehensive study was performed by Parak and colleagues (56), who determined the hydrodynamic radii of the QDs, in both organic solvents and water, and also characterized their diffusion behavior in complex fluids such as actin solutions to prove their potential per se for biological applications.

Binding. Any changes in molecular shape or size that affect the hydrodynamic radius of the particle are reflected in the diffusion coefficient and thus in the average diffusion time. However, the diffusion coefficient depends on the hydrodynamic radius, which is proportional to the cubic root of the molecular mass for a spherical particle. This means that a homogenous increase in mass by a factor of 8 only doubles the diffusion time.

In vitro. Octobre et al. (66) recently applied this technique to study the interaction of a transcription factor with its DNA target sequence. Binding of the protein to the DNA resulted in significant changes of the diffusion, so that the apparent equilibrium dissociation constant K_D could be estimated from a concentration series (66). Nomura et al. (65) tested the feasibility of rapid detection of oxidative damage of mitochondrial DNA by FCS. Analysis times of 5 min (compared to 3 h with conventional methods) are promising for future diagnostic applications. To investigate unlabeled protein, researchers bind the substrate to small fluorescent spheres and monitor their diffusion behavior. In this way the Walla group (68) investigated the interaction of lectins with carbohydrated fluorescent nanobeads. If the binding reaction does not entail a sufficient increase in mass, one of the reaction partners can be attached to nonfluorescent nanospheres (2) or small lipid vesicles (75).

In artificial membranes. In more complex environments, the diffusion coefficient may depend even less on the size of the molecular complex. In membranes, this is determined by the Saffman-Delbrück equation for molecules that are larger than a single lipid:

$$D = \frac{k \cdot T}{4\pi \cdot \eta_{membrane} \cdot h} \cdot \left(\ln \frac{\eta_{membrane} \cdot h}{\eta_{medium} \cdot R} - \gamma \right) \quad \text{with} \quad \text{Euler's constant } \gamma = 0.5772. \qquad 14.$$

Here, T is the temperature, k is Boltzmann's constant, $\eta_{membrane}$ is the membrane viscosity, η_{medium} is the viscosity of the exterior medium, h is the membrane thickness, and R is the (lateral) radius of the particle.

Owing to logarithmic dependence, diffusion experiments on membranes are typically restricted to study the lipid microenvironment—and hence the local viscosity—rather than binding reactions. The existence of small-lipid microdomains, termed rafts, in artificial and cellular membranes has been studied extensively. Bacia et al. (5) investigated artificial membranes (giant unilamellar vesicles, GUVs) with different lipid compositions and demonstrated the quantitative effects of cholesterol depletion on the diffusion properties of special marker molecules (**Figure 3**). A two-channel setup allows one to monitor simultaneously spectrally distinct membrane probes with different partition properties to reveal potential submicroscopic membrane heterogeneities (50).

In vivo. However, both the outer shell and the interior of living cells are crowded and thus much more complicated than any in vitro situation. Wang et al. (83) employed TPE to study Cdc20, an important mitotic checkpoint protein, throughout the cell cycle and monitored the underlying periodic pattern of association with and dissociation from APC/C (anaphase-promoting complex or cyclosome). The observed changes in the biochemical assembly states of Cdc20 correlate well with the known temporal pattern of the activity of APC/C_{Cdc20} in mitosis (83). Maertens et al. (58), on the other hand, applied single-color FCS to investigate the interaction of the EGFP fusion proteins HIV-1 integrase and lens epithelium-derived growth factor/transcription coactivator p75 (LEDGF/p75) by the change in diffusion coefficient upon binding. Even more complex is the system presented by Bernacchi et al. (10). They characterized the infection entry pathway of simian virus 40 into cells. Both the formation of caveolae after viral infection and the subsequent diffusion of caveosome vesicles in

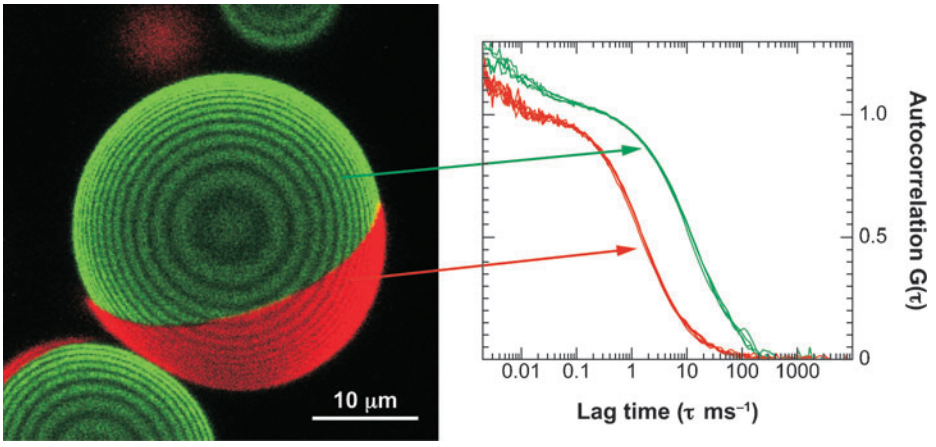

Figure 3

Giant unilamellar vesicle (GUV) showing phase separation into a liquid-ordered (*green*) and liquid-disordered phase (*red*). Domains have been visualized with specific markers, diI (*red*) and Alexa488-labeled cholera toxin B-subunit bound to GM1 (*green*). Diffusion of the marker is significantly slower in the liquid-ordered phase than in the liquid-disordered phase. Images and data courtesy of K. Bacia.

the cytoplasm are demonstrated, followed by the capsid disassembly.

FRET: fluorescence resonance energy transfer

Molecular structure. The effects of conformational rearrangements on the diffusion coefficient are minute. Nevertheless, it is possible to show that propidium iodide, a rather common DNA-intercalating dye, alters its conformation (51), and to monitor the unfolding of proteins induced by guanidinium hydrochloride (18).

Fluctuations. Mobility-related information can generally be found on the longest timescales accessible by FCS, but FCS is sensitive to any correlated change in molecular brightness during the molecule's transit through the laser beam. The most prominent, nearly omnipresent brightness fluctuations are caused by transitions of the fluorophores to the triplet state, which depend, for example, on the excitation power and mode or on the presence of quenching molecules such as oxygen (20, 37). These light-induced processes generally occur on microsecond timescales, as do isomerization processes (86).

The family of green fluorescent proteins is known for pH-induced flickering due to a shift in the absorption spectrum in the protonated state, which renders it effectively nonexcitable at a given wavelength (32). Conformational fluctuations can be monitored with suitable fluorescent markers that are quenched in the proximity of the protein (17).

On even shorter timescales, this principle can be extended to quantify fluorescence resonance energy transfer (FRET) by actively introducing a second dye as an acceptor or an efficient quencher (31). In DNA, intrinsic guanosine residues work well to examine the dynamics of hairpin folding (45). When polarized excitation, detection, or both are used, rotational Brownian motions also can be visualized. Depending on the particle size, rotational correlation times range from ~20 ns for GFP to ~1 μs for large semiconductor nanorods or DNA complexes (84).

Photon antibunching, which is directly related to the fluorescence lifetime of the chromophore, is the fastest process accessible by FCS. This information has been used recently to study inclusion complexes of pyronines with cyclodextrin (1, 30).

Dual-Channel Applications: FCCS

However, dual-channel applications are much more versatile and offer more than twice the information accessible from one-channel measurements.

Dual-color FCCS. By dual-color fluorescence cross-correlation spectroscopy (dcFCCS) it is possible to compare two spectrally distinct chromophores, whereas spatial FCCS highlights similarities between two distinct regions in the sample.

Two-color excitation. Different colored fluorescence tags are excited by two superimposed laser beams (OPE). This technique has been applied successfully in vitro to monitor DNA-hybridization and enzyme kinetics (77) and to investigate ligand or drug binding. Recent applications comprise the development of a new, sensitive DNA recombination assay intended to facilitate the discovery of novel stable DNA biomolecular tools for site-specific exchange of genetic information (42). Rigler & Meier (71) report another, more medical application, the successful encapsulation of fluorophores by functionalized nanocontainers as potential drug delivery systems. Especially for intracellular applications, fusions of autofluorescent proteins with proteins that are investigated in the living cell can be cloned and expressed in the organism. This genetic labeling has a variety of benefits. Not only is the labeling efficiency 100%, but transfection of the cells with the labeled compounds is no longer necessary, so that no residual native protein has to be accounted for. Two studies were performed by Baudendistel et al. (6), who showed the in vivo binding of Fos and Jun, two components of the AP-1 transcription factor, and our group (48), who investigated caspase-3 activity on specifically designed all-protein substrate molecules. Both studies feature EGFP and mRFP; the latter is also using rsGFP and *tdimer2(12)*.

One-color excitation. Earlier, Kohl et al. (49) showed that these proteins are also ideally suited for multiphoton excitation (MPE), but QDs might be a viable alternative despite their size (53). Swift et al. (80) have applied QDs to a model ligand-receptor system. To date, synthetic chromophores or autofluorescent proteins still prevail.

Berland (7) is using green- and red-labeled, short single-stranded DNA to detect the concentration of a third, unlabeled strand that has specific sequences complementary to both of the labeled short strands. Another ternary reaction has been shown by Merkle et al. (62), who analyzed DNA synapsis and end joining in solution to study repair mechanisms for DNA double-strand breaks by monitoring the fusion of red- and green-labeled oligonucleotides by unlabeled proteins. Collini et al. (19) even proposed this technique as a potential tool for high-throughput screening of DNA repair activity, using base-excision repair as a model assay. Biomolecules do not necessarily bind at a one-to-one ratio. Although long thought to be too complex, the stoichiometry of more complicated reactions may be assessed (46).

If the longer-wavelength dye exhibits an unusually large Stokes shift, two spectrally distinct chromophores can be excited with one visible continuous wave laser line (41). One-color excitation is also required to excite the donor of a FRET pair. Using a global analysis of the data recorded simultaneously in the donor and acceptor channel, in addition to the corresponding cross-correlation, Eggeling et al. (25) demonstrated the potential of two-color global FCS (2CG-FCS) for FRET samples and also suppressed unwanted artifacts.

Background suppression. Other methods of background reduction rely on the different fluorescence lifetimes of sample molecules and impurities. In 2000, Lamb et al. (52) presented a way to implement lifetime gating in FCS experiments. Using a pulsed laser as an excitation source and a laser-synchronized gate in the detection channel, the authors suppressed photons emitted within a certain time interval after excitation.

FCCS: fluorescence cross-correlation spectroscopy

MPE: multiphoton excitation

SFCS: scanning fluorescence correlation spectroscopy

This principle, known as pulsed interleaved excitation (PIE) (64) or cross-talk-free FCCS (81), has been extended to two excitation and detection channels to reduce spectral cross talk. The sample is excited with alternating green and red ultrashort laser pulses. The alternating frequency is significantly longer than the fluorescence lifetime of the chromophores, so that the chance of detecting unwanted stray photons in the subsequent excitation and detection interval—attributed to the other color—is negligible.

Spatial FCCS. Alternating the excitation power between two spatially distinct laser foci also is an excellent way to reduce spatial excitation cross talk and to highlight molecules simultaneously moving at specific velocities. Most frequently, spatial FCCS is used to map flow rates in microfluidic devices with high spatial resolution (24). Two separate beams may also trigger reactions, e.g., the first beam photoconverts the fluorescent protein Kaede and the second beam probes the effects (23), and thus utilize flow to achieve high time resolutions. In this way FRET reactions can be followed using a dual-color dual-focus setup with four detection channels (22).

Beyond Traditional FCS

In recent years, these rather traditional basic FCS concepts have been extended to a vast family of FCS-related methods.

Multichannel experiments. Most biochemical reactions involve three or more components. In order for these reactions to be examined, more than two components must be monitored at any given time. Our group (34) first demonstrated the simultaneous TPE of three distinct chromophores. Using triple-color coincidence analysis, we showed the scope of this method with a simple nucleic acid model system. Three chromophores with a suitable Stokes shift can also be excited by OPE (39). Additional colors can be distinguished by using more flexible grating- or prism-based detection platforms for multicolor applications (13, 40).

Increasing the number of spatial channels is not as straightforward because the number of individual laser foci and APDs monitoring them is finite. One method to create an array of focal volumes consists of using 2×2 fan-out diffractive optical elements and an array of APDs or one single-photon 2×2 CMOS (complementary metal-oxide-semiconductor) detector array (11). However, to cover larger regions, epifluorescence or total internal reflection fluorescence (TIRF) excitation is employed and detector arrays are exchanged for highly sensitive CCD cameras (14, 43), in which individual pixels act as pinholes (**Figure 4**). This is a first step to combining single-point FCS with high temporal resolution and image correlation spectroscopy with access to long diffusion times and spatially resolved dynamic information. Digman et al. (21) presented another way to achieve this goal. Using a standard laser-scanning microscope, they exploited the hidden time structure of the scan method, i.e., the microsecond time delay between adjacent pixels, to record processes on timescales of microseconds to seconds (21). Raster image correlation spectroscopy allows one to access the temporal resolution of single-point FCS while retaining the spatial information provided by the imaging technique. The first experimental results show the spatially resolved diffusions of paxillin-EGFP in CHO-K1 cells.

Scanning FCS. Science has now come full circle, because image correlation spectroscopy was originally introduced as an extension of the established concept of scanning FCS (SFCS) (67). The idea of performing FCS measurements while scanning the laser beam across the sample or vice versa to determine molar weights and lateral diffusion constants of rather immobile particles dates back 20 years (63). Berland et al. (8) extended this concept to MPE to characterize molecular aggregates. Sample scanning

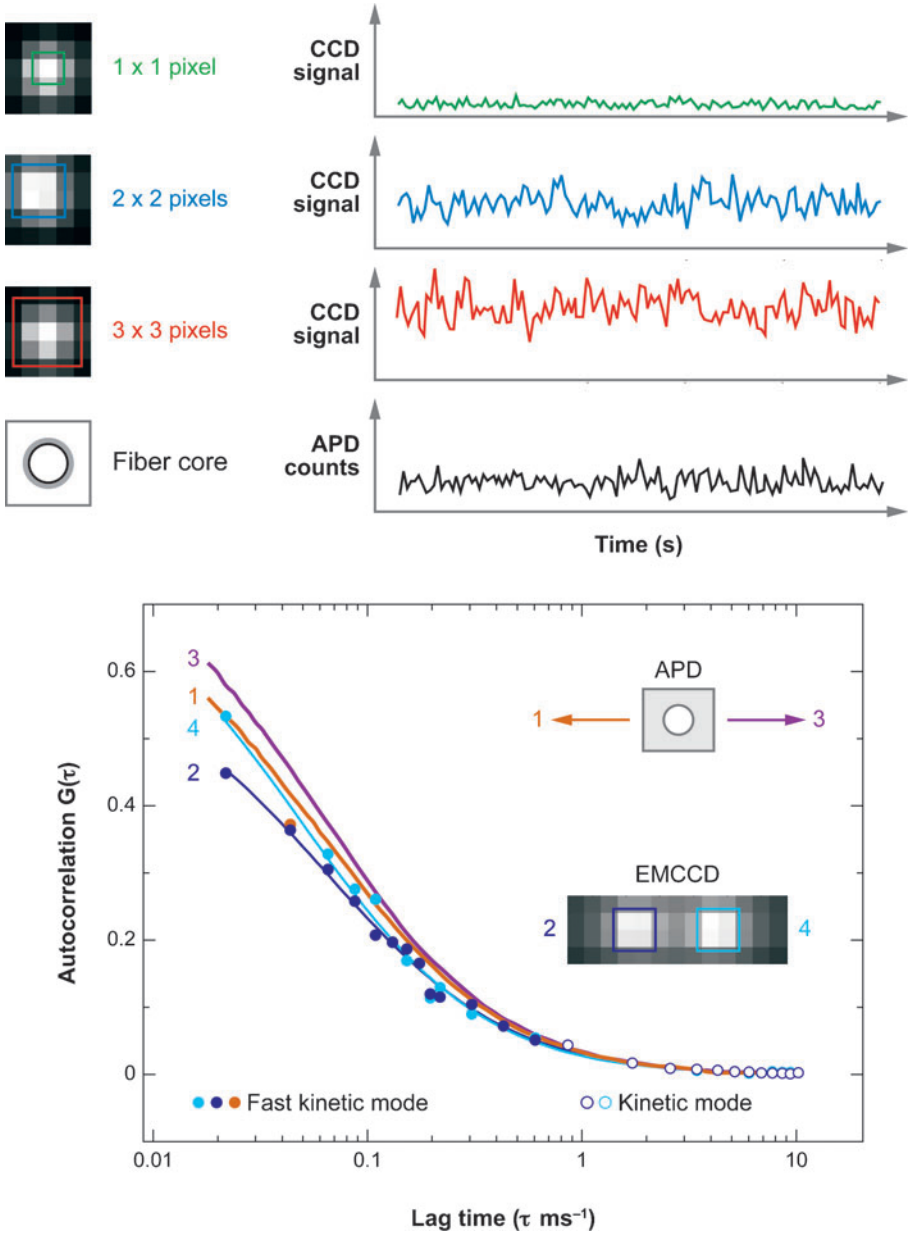

Figure 4

Top: Schematic dependence of the fluorescence signal (*top right*) for different integration regions on the CCD chip (*top left*). The pixel size is 24 × 24 μm. As the sensitive area increases, so does the average signal. The bottom trace (*black*) originates from a standard APD measurement with an optical fiber (50 μm in diameter) and is sketched for comparison. Bottom: Comparison of FCS curves recorded simultaneously in two different locations (two-spot FCS) for Alexa488 using the CCD [curves 2 (*blue*) and 4 (*cyan*), symbols and solid line fit curves] and successively by an APD [curves 1 (*orange*) and 3 (*purple*), solid lines]. Data obtained with fast kinetics mode are drawn as closed circles. The fit results, especially the diffusion times, agree well within the accuracy of the experiment (cf. Reference 14). Figure courtesy of M. Burkhardt.

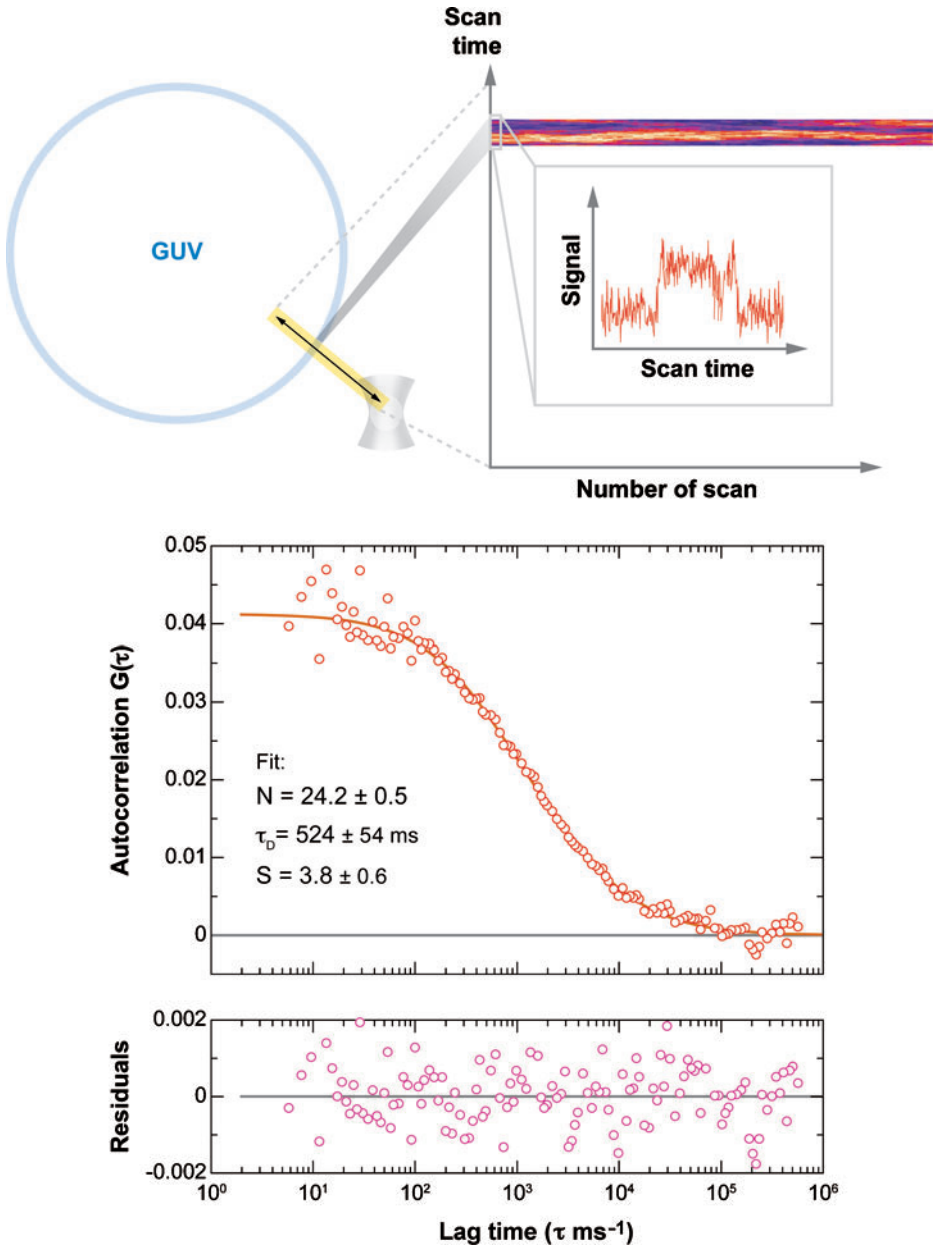

Figure 5

Top: A schematic depicting the principle of SFCS. A series of line scans is performed perpendicular to the membrane in the equatorial plane of the GUV (*top left*). The data for each scan are arranged in a column (*top right*), where the membrane can be seen as a bright region. The relative position of individual columns can be shifted to correct for membrane movements. Bottom: SFCS curve for Alexa488-labeled B-subunit of choleratoxin B bound to GM1 in the GUV membrane. Data (*red open circles*) were acquired for 20 min at a repetition rate of 520 Hz and scan speed of 0.14 m s^{-1}. Data were analyzed combining a diffusion model with directed flow (cf. Reference 72). Data courtesy of J. Ries.

combined with dual-color excitation and detection can be employed to distinguish binding from mere accidental colocalization below the optical resolution limit (3).

If a laser beam is directed across a sample in a repetitive fashion, the spatially encoded information may be used to calculate multiple FCS curves at specific positions along the beam path (73). For points along a circular scan trajectory, the phase angle is sufficient for unequivocal identification. Therefore, correlations can be calculated as a function of lag time and phase (position-sensitive SFCS) (79). The scan rate must be significantly faster than the molecular motions of interest, which makes this technique ideal for membrane applications, especially because external FCS detection units can be added to some commercial laser-scanning microscopes (70). One option for SFCS performed by our group is depicted in **Figure 5**.

Resolution enhancements. The spatial resolution of FCS is restricted by the diffraction limit, but there are strategies to partially overcome these limitations. Heterogeneities caused by subwavelength structures such as membrane rafts are simply averaged out if the resolution is not increased. Elaborate experimental and theoretical studies show the change in diffusion properties of a putative raft marker and a transmembrane protein relative to variations in the size of the illuminated area (54). This finding allows conclusions regarding the nature of a potential confinement. Alternatively, z-scan FCS is applied to gain information on potential microdomains in membranes (38). Here the observation area, i.e., the cross-section of the laser beam exciting the membrane, can be varied simply by performing a z-scan through the membrane.

The size of the observation volume also restricts FCS to dye concentrations in the submicromolar range, but equilibrium binding constants sometimes exceed this range and thus require smaller focal volumes. The apparent observation volume can be reduced by using nanostructured surfaces. Subwavelength apertures milled in, for example, gold films are used to both increase spatial resolution and enhance detected fluorescence (55). These zero-mode waveguides allow a dramatic increase in the accessible concentration range (76).

TIR: total internal reflection

The illuminated region can also be restricted solely by optical means, mainly by total internal reflection (TIR) (82), but more recently also by stimulated emission depletion (STED) (44). Whereas STED offers a fivefold compaction of the focal volume, a reduction by almost two orders of magnitude has been reported with TIRFM (74). Established by Thompson et al. (82) in 1981, TIR-FCS lay dormant for nearly two decades after some promising initial applications on surface-binding rates of biomolecules. In 1999, it was applied to supported lipid bilayers (12) and later to receptor-ligand interactions, even with nonfluorescent competitors (57). TIR-FCS is restricted to surface measurements with a maximum illumination depth of about 200 nm, which means that only the axial resolution is increased inherently, whereas lateral resolution is enforced by pinholes. STED causes a more uniform reduction of the illuminated region in all three dimensions, and it can be applied in solution (44). Thus, intracellular measurements also seem feasible despite the rather high laser intensities required.

CONCLUSIONS

FCS looks back on a long and busy history. During the past 10 years, it has evolved into an umbrella term for numerous individual applications, so that FCS can be counted among the standard techniques for biophysical in vitro and in vivo measurements. FCS has proven to be a stable, reliable, and minimally invasive technique that can be adapted to a myriad of environmental and sample conditions. With multicolor applications, high spatial and temporal resolution, and multiplexing, it should be possible to find an ideal FCS variety for nearly any problem.

SUMMARY POINTS

1. FCS is a versatile technique that has become a standard method to monitor molecular interactions in vivo and in vitro.
2. Single-channel measurements highlight photophysical phenomena, conformational changes, and mobility-related parameters.
3. Binding studies can be performed by OPE and MPE using multichannel detection and multicolor cross-correlation.
4. SFCS, raster image correlation spectroscopy, and image correlation spectroscopy extend the accessible time range as far as seconds.
5. Spatial resolution can be enhanced by clever mathematical extrapolation, TIR-FCS, and STED-FCS.

ACKNOWLEDGMENTS

The authors are grateful to Kirsten Bacia, Thomas Ohrt, and Markus Burkhardt for helpful discussions and to the Volkswagen Foundation for financial support.

LITERATURE CITED

1. Al Soufi W, Reija B, Novo M, Felekyan S, Kühnemuth R, Seidel CAM. 2005. Fluorescence correlation spectroscopy, a tool to investigate supramolecular dynamics: inclusion complexes of pyronines with cyclodextrin. *J. Am. Chem. Soc.* 127:8775–84
2. Allen NW, Thompson NL. 2006. Ligand binding by estrogen receptor beta attached to nanospheres measured by fluorescence correlation spectroscopy. *Cytometry* 69A:524–32
3. Amediek A, Haustein E, Scherfeld D, Schwille P. 2002. Scanning dual-color cross-correlation analysis for dynamic colocalization studies of immobile molecules. *Single Mol.* 3:201–10
4. Aragón SR, Pecora R. 1975. Fluorescence correlation spectroscopy and Brownian rotational diffusion. *Biopolymers* 14:119–38
5. Bacia K, Scherfeld D, Kahya N, Schwille P. 2004. Fluorescence correlation spectroscopy relates rafts in model and native membranes. *Biophys. J.* 87:1034–43
6. Baudendistel N, Müller G, Waldeck W, Angel P, Langowski J. 2005. Two-hybrid fluorescence cross-correlation spectroscopy detects protein-protein interactions in vivo. *Chemphyschem* 6:984–90
7. Berland KM. 2004. Detection of specific DNA sequences using dual-color two-photon fluorescence correlation spectroscopy. *J. Biotechnol.* 108:127–36
8. Berland KM, So PT, Chen Y, Mantulin WW, Gratton E. 1996. Scanning two-photon fluctuation correlation spectroscopy: particle counting measurements for detection of molecular aggregation. *Biophys. J.* 71:410–20
9. Berland KM, So PT, Gratton E. 1995. Two-photon fluorescence correlation spectroscopy: method and application to the intracellular environment. *Biophys. J.* 68:694–701
10. Bernacchi S, Mueller G, Langowski J, Waldeck W. 2004. Characterization of simian virus 40 on its infectious entry pathway in cells using fluorescence correlation spectroscopy. *Biochem. Soc. Trans.* 32:746–49

11. Blom H, Johansson M, Gosch M, Sigmundsson T, Holm J, et al. 2002. Parallel flow measurements in microstructures by use of a multifocal 4 × 1 diffractive optical fan-out element. *Appl. Opt.* 41:6614–20
12. Broek WV, Huang Z, Thompson NL. 1999. High-order autocorrelation with imaging fluorescence correlation spectroscopy: application to IgE on supported planar membranes. *J. Fluoresc*. 9:313–24
13. Burkhardt M, Heinze KG, Schwille P. 2005. Four-color fluorescence correlation spectroscopy realized in a grating-based detection platform. *Opt. Lett*. 30:2266–68
14. Burkhardt M, Schwille P. 2006. Electron multiplying CCD based detection for spatially resolved fluorescence correlation spectroscopy. *Opt. Exp*. 14:5013–20
15. Campbell RE, Tour O, Palmer AE, Steinbach PA, Baird GS, et al. 2002. A monomeric red fluorescent protein. *Proc. Natl. Acad. Sci. USA* 99:7877–82
16. Charier S, Meglio A, Alcor D, Cogne-Laage E, Allemand JF, et al. 2005. Reactant concentrations from fluorescence correlation spectroscopy with tailored fluorescent probes. An example of local calibration-free pH measurement. *J. Am. Chem. Soc.* 127:15491–505
17. Chattopadhyay K, Elson EL, Frieden C. 2005. The kinetics of conformational fluctuations in an unfolded protein measured by fluorescence methods. *Proc. Natl. Acad. Sci. USA* 102:2385–89
18. Chattopadhyay K, Saffarian S, Elson EL, Frieden C. 2005. Measuring unfolding of proteins in the presence of denaturant using fluorescence correlation spectroscopy. *Biophys. J.* 88:1413–22
19. Collini M, Caccia M, Chirico G, Barone F, Dogliotti E, Mazzei F. 2005. Two-photon fluorescence cross-correlation spectroscopy as a potential tool for high-throughput screening of DNA repair activity. *Nucleic Acids Res.* 33:e165
20. Cotlet M, Goodwin PM, Waldo GS, Werner JH. 2006. A comparison of the fluorescence dynamics of single molecules of a green fluorescent protein: one- versus two-photon excitation. *Chemphyschem* 7:250–60
21. Digman MA, Brown CM, Sengupta P, Wiseman PW, Horwitz AR, Gratton E. 2005. Measuring fast dynamics in solutions and cells with a laser scanning microscope. *Biophys. J.* 89:1317–27
22. Dittrich PS, Müller B, Schwille P. 2004. Studying reaction kinetics by simultaneous FRET and cross-correlation analysis in a miniaturized continuous flow reactor. *Phys. Chem. Chem. Phys*. 6:4416–20
23. Dittrich PS, Schäfer SP, Schwille P. 2005. Characterization of the photoconversion on reaction of the fluorescent protein Kaede on the single-molecule level. *Biophys. J.* 89:3446–55
24. Dittrich PS, Schwille P. 2002. Spatial two-photon fluorescence cross-correlation spectroscopy for controlling molecular transport in microfluidic structures. *Anal. Chem*. 74:4472–79
25. Eggeling C, Kask P, Winkler D, Jäger S. 2005. Rapid analysis of Forster resonance energy transfer by two-color global fluorescence correlation spectroscopy: trypsin proteinase reaction. *Biophys. J.* 89:605–18
26. Elson EL, Magde D. 1974. Fluorescence correlation spectroscopy. I. Conceptual basis and theory. *Biopolymers* 13:1–27
27. Elson EL, Schlessinger J, Koppel DE, Axelrod D, Webb WW. 1976. Measurement of lateral transport on cell surfaces. *Prog. Clin. Biol. Res*. 9:137–47
28. Enderlein J, Gregor I, Patra D, Fitter J. 2005. Statistical analysis of diffusion coefficient determination by fluorescence correlation spectroscopy. *J. Fluoresc*. 15:415–22

29. Fahey PF, Barak LS, Elson EL, Koppel DE, Wolf DE, Webb WW. 1977. Lateral diffusion in planar lipid bilayers. *Science* 195:305–6
30. Felekyan S, Kühnemuth R, Kudryavtsev V, Sandhagen C, Becker W, Seidel CA. 2005. Full correlation from picoseconds to seconds by time-resolved and time-correlated single photon detection. *Rev. Sci. Instrum.* 76:83104
31. Gopich I, Szabo A. 2005. Fluorophore-quencher distance correlation functions from single-molecule photon arrival trajectories. *J. Phys. Chem. B* 109:6845–48
32. Haupts U, Maiti S, Schwille P, Webb WW. 1998. Dynamics of fluorescence fluctuations in green fluorescent protein observed by fluorescence correlation spectroscopy. *Proc. Natl. Acad. Sci. USA* 95:13573–78
33. Haustein E, Schwille P. 2007. Fluorescence correlation spectroscopy: a versatile technique with single-molecule sensitivity. In *Light Scattering-Fluctuation and Grating Techniques*, ed. R Pecora, R Borsali, 2: In press. Dordrecht, The Neth.: Kluwer Academic. 1st ed.
34. Heinze KG, Jahnz M, Schwille P. 2004. Triple-color coincidence analysis: one step further in following higher order molecular complex formation. *Biophys. J.* 86:506–16
35. Heinze KG, Rarbach M, Jahnz M, Schwille P. 2002. Two-photon fluorescence coincidence analysis: rapid measurements of enzyme kinetics. *Biophys. J.* 83:1671–81
36. Hess ST, Webb WW. 2002. Focal volume optics and experimental artifacts in confocal fluorescence correlation spectroscopy. *Biophys. J.* 83:2300–17
37. Hübner CG, Renn A, Renge I, Wild UP. 2001. Direct observation of the triplet lifetime quenching of single dye molecules by molecular oxygen. *J. Chem. Phys.* 115:9619–22
38. Humpolickova J, Gielen E, Benda A, Fagulova V, Vercammen J, et al. 2006. Probing diffusion laws within cellular membranes by Z-scan fluorescence correlation spectroscopy. *Biophys. J.* 91:L23–25
39. Hwang LC, Gosch M, Lasser T, Wohland T. 2006. Simultaneous multicolor fluorescence cross-correlation spectroscopy to detect higher order molecular interactions using single wavelength laser excitation. *Biophys. J.* 91:715–27
40. Hwang LC, Leutenegger M, Gosch M, Lasser T, Rigler P, et al. 2006. Prism-based multicolor fluorescence correlation spectrometer. *Opt. Lett.* 31:1310–12
41. Hwang LC, Wohland T. 2004. Dual-color fluorescence cross-correlation spectroscopy using single laser wavelength excitation. *Chemphyschem* 5:549–51
42. Jahnz M, Schwille P. 2005. An ultrasensitive site-specific DNA recombination assay based on dual-color fluorescence cross-correlation spectroscopy. *Nucleic Acids Res.* 33:e60
43. Kannan B, Har JY, Liu P, Maruyama I, Ding JL, Wohland T. 2006. Electron multiplying charge-coupled device camera based fluorescence correlation spectroscopy. *Anal. Chem.* 78:3444–51
44. Kastrup L, Blom H, Eggeling C, Hell SW. 2005. Fluorescence fluctuation spectroscopy in subdiffraction focal volumes. *Phys. Rev. Lett.* 9417:8104
45. Kim J, Doose S, Neuweiler H, Sauer M. 2006. The initial step of DNA hairpin folding: a kinetic analysis using fluorescence correlation spectroscopy. *Nucleic Acids Res.* 34:2516–27
46. Kim SA, Heinze KG, Bacia K, Waxham MN, Schwille P. 2005. Two-photon cross-correlation analysis of intracellular reactions with variable stoichiometry. *Biophys. J.* 88:4319–36
47. Kinjo M, Rigler R. 1995. Ultrasensitive hybridization analysis using fluorescence correlation spectroscopy. *Nucleic Acids Res.* 23:1795–99
48. Kohl T, Haustein E, Schwille P. 2005. Determining protease activity in vivo by fluorescence cross-correlation analysis. *Biophys. J.* 89:2770–82

49. Kohl T, Heinze KG, Kuhlemann R, Koltermann A, Schwille P. 2002. A protease assay for two-photon cross-correlation and FRET analysis based solely on fluorescent proteins. *Proc. Natl. Acad. Sci. USA* 99:12161–66
50. Korlach J, Baumgart T, Webb WW, Feigenson GW. 2005. Detection of motional heterogeneities in lipid bilayer membranes by dual probe fluorescence correlation spectroscopy. *Biochim. Biophys. Acta* 1668:158–63
51. Kral T, Widerak K, Langner M, Hof M. 2005. Propidium iodide and PicoGreen as dyes for the DNA fluorescence correlation spectroscopy measurements. *J. Fluoresc.* 15:179–83
52. Lamb DC, Schenk A, Röcker C, Scalfi-Happ C, Nienhaus GU. 2000. Sensitivity enhancement in fluorescence correlation spectroscopy of multiple species using time-gated detection. *Biophys. J.* 79:1129–38
53. Larson DR, Zipfel WR, Williams RM, Clark SW, Bruchez MP, et al. 2003. Water-soluble quantum dots for multiphoton fluorescence imaging in vivo. *Science* 300:1434–36
54. Lenne PF, Wawrezinieck L, Conchonaud F, Wurtz O, Boned A, et al. 2006. Dynamic molecular confinement in the plasma membrane by microdomains and the cytoskeleton meshwork. *EMBO J.* 25:3245–56
55. Leutenegger M, Gosch M, Perentes A, Hoffmann P, Martin OJF, Lasser T. 2006. Confining the sampling volume for fluorescence correlation spectroscopy using a subwavelength sized aperture. *Optics Exp.* 14:956–69
56. Liedl T, Keller S, Simmel FC, Rädler JO, Parak WJ. 2005. Fluorescent nanocrystals as colloidal probes in complex fluids measured by fluorescence correlation spectroscopy. *Small* 1:997–1003
57. Lieto AM, Thompson NL. 2004. Total internal reflection with fluorescence correlation spectroscopy: nonfluorescent competitors. *Biophys. J.* 87:1268–78
58. Maertens G, Vercammen J, Debyser Z, Engelborghs Y. 2005. Measuring protein-protein interactions inside living cells using single color fluorescence correlation spectroscopy. Application to human immunodeficiency virus type I integrase and LEDGF/p75. *FASEB J.* 19:1039–41
59. Magde D, Elson EL, Webb WW. 1974. Fluorescence correlation spectroscopy. II. An experimental realization. *Biopolymers* 13:29–61
60. Magde D, Elson EL, Webb WW. 1972. Thermodynamic fluctuations in a reacting system: measurement by fluorescence correlation spectroscopy. *Phys. Rev. Lett.* 29:705–8
61. Magde D, Webb WW, Elson EL. 1978. Fluorescence correlation spectroscopy. III. Uniform translation and laminar flow. *Biopolymers* 17:361–76
62. Merkle D, Block WD, Yu Y, Lees-Miller SP, Cramb DT. 2006. Analysis of DNA-dependent protein kinase-mediated DNA end joining by two-photon fluorescence cross-correlation spectroscopy. *Biochemistry* 45:4164–72
63. Meyer T, Schindler H. 1988. Particle counting by fluorescence correlation spectroscopy. Simultaneous measurement of aggregation and diffusion of molecules in solutions and in membranes. *Biophys. J.* 54:983–93
64. Müller BK, Zaychikov E, Bräuchle C, Lamb DC. 2005. Pulsed interleaved excitation. *Biophys. J.* 89:3508–22
65. Nomura Y, Fuchigami H, Kii H, Feng ZG, Nakamura T, Kinjo M. 2006. Detection of oxidative stress-induced mitochondrial DNA damage using fluorescence correlation spectroscopy. *Anal. Biochem.* 350:196–201
66. Octobre G, Lemercier C, Khochbin S, Robert-Nicoud M, Souchier C. 2005. Monitoring the interaction between DNA and a transcription factor (MEF2A) using fluorescence correlation spectroscopy. *C. R. Biol.* 328:1033–40

67. Petersen NO, Hoddelius PL, Wiseman PW, Seger O, Magnusson KE. 1993. Quantitation of membrane receptor distributions by image correlation spectroscopy: concept and application. *Biophys. J.* 65:1135–46
68. Pohl WH, Hellmuth H, Hilbert M, Seibel J, Walla PJ. 2006. A two-photon fluorescence-correlation study of lectins interacting with carbohydrated 20 nm beads. *Chembiochem* 7:268–74
69. Rauer B, Neumann E, Widengren J, Rigler R. 1996. Fluorescence correlation spectrometry of the interaction kinetics of tetramethylrhodamin alpha-bungarotoxin with *Torpedo californica* acetylcholine receptor. *Biophys. Chem.* 58:3–12
70. Ries J, Schwille P. 2006. Studying slow membrane dynamics with continuous wave scanning fluorescence correlation spectroscopy. *Biophys. J.* 91:1915–24
71. Rigler P, Meier W. 2006. Encapsulation of fluorescent molecules by functionalized polymeric nanocontainers: investigation by confocal fluorescence imaging and fluorescence correlation spectroscopy. *J. Am. Chem. Soc.* 128:367–73
72. Rigler R, Mets U, Widengren J, Kask P. 1993. Fluorescence correlation spectroscopy with high count rate and low background analysis of translational diffusion. *Eur. Biophys. J.* 22:169–75
73. Ruan QQ, Cheng MA, Levi M, Gratton E, Mantulin WW. 2004. Spatial-temporal studies of membrane dynamics: scanning fluorescence correlation spectroscopy (SFCS). *Biophys. J.* 87:1260–67
74. Ruckstuhl T, Seeger S. 2004. Attoliter detection volumes by confocal total-internal-reflection fluorescence microscopy. *Opt. Lett.* 29:569–71
75. Rusu L, Gambhir A, McLaughlin S, Rädler J. 2004. Fluorescence correlation spectroscopy studies of peptide and protein binding to phospholipid vesicles. *Biophys. J.* 87:1044–53
76. Samiee KT, Moran-Mirabal JM, Cheung YK, Craighead HG. 2006. Zero mode waveguides for single-molecule spectroscopy on lipid membranes. *Biophys. J.* 90:3288–99
77. Schwille P, Meyer-Almes FJ, Rigler R. 1997. Dual-color fluorescence cross-correlation spectroscopy for multicomponent diffusional analysis in solution. *Biophys. J.* 72:1878–86
78. Shaner NC, Campbell RE, Steinbach PA, Giepmans BN, Palmer AE, Tsien RY. 2004. Improved monomeric red, orange and yellow fluorescent proteins derived from *Discosoma* sp. red fluorescent protein. *Nat. Biotechnol.* 22:1567–72
79. Skinner JP, Chen Y, Müller JD. 2005. Position-sensitive scanning fluorescence correlation spectroscopy. *Biophys. J.* 89:1288–301
80. Swift JL, Heuff R, Cramb DT. 2006. A two-photon excitation fluorescence cross-correlation assay for a model ligand-receptor binding system using quantum dots. *Biophys. J.* 90:1396–410
81. Thews E, Gerken M, Eckert R, Zapfel J, Tietz C, Wrachtrup J. 2005. Cross talk free fluorescence cross correlation spectroscopy in live cells. *Biophys. J.* 89:2069–76
82. Thompson NL, Burghardt TP, Axelrod D. 1981. Measuring surface dynamics of biomolecules by total internal reflection fluorescence with photobleaching recovery or correlation spectroscopy. *Biophys. J.* 33:435–54
83. Wang ZF, Shah JV, Berns MW, Cleveland DW. 2006. In vivo quantitative studies of dynamic intracellular processes using fluorescence correlation spectroscopy. *Biophys. J.* 91:343–51
84. Widengren J, Mets U, Rigler R. 1999. Photodynamic properties of green fluorescent proteins investigated by fluorescence correlation spectroscopy. *Chem. Phys.* 250:171–86
85. Widengren J, Rigler R. 1998. Fluorescence correlation spectroscopy as a tool to investigate chemical reactions in solutions and on cell surfaces. *Cell Mol. Biol.* 44:857–79

86. Widengren J, Seidel CA. 2000. Manipulation and characterization of photo-induced transient states of merocyanine 540 by fluorescence correlation spectroscopy. *Phys. Chem. Chem. Phys.* 2:3435–41
87. Yu LL, Tan MY, Ho B, Ding JL, Wohland T. 2006. Determination of critical micelle concentrations and aggregation numbers by fluorescence correlation spectroscopy: aggregation of a lipopolysaccharide. *Anal. Chim. Acta* 556:216–25
88. Zhang PD, Li LA, Dong CQ, Qian HF, Ren JC. 2005. Sizes of water-soluble luminescent quantum dots measured by fluorescence correlation spectroscopy. *Anal. Chim. Acta* 546:46–51

Annual Review of Biophysics and Biomolecular Structure

Volume 35, 2006

Contents